



# Quantifying SO<sub>2</sub> oxidation pathways to atmospheric sulfate using stable sulfur and oxygen isotopes: laboratory simulation and field observation

Ziyan Guo<sup>1</sup>, Keding Lu<sup>1</sup>, Pengxiang Qiu<sup>2</sup>, Mingyi Xu<sup>2</sup>, and Zhaobing Guo<sup>2</sup>

<sup>1</sup>State Key Joint Laboratory of Environmental Simulation and Pollution Control, State Environmental Protection Key Laboratory of Atmospheric Ozone Pollution Control, College of Environmental Sciences and Engineering, Peking University, Beijing 100871, China

<sup>2</sup>Jiangsu Key Laboratory of Atmospheric Environment Monitoring and Pollution Control (AEMPC), Collaborative Innovation Center of Atmospheric Environment and Equipment Technology (CIC-AEET), School of Environmental Science and Engineering, Nanjing University of Information Science and Technology, Nanjing 210044, China

**Correspondence:** Keding Lu (k.lu@pku.edu.cn) and Zhaobing Guo (guocumt@nuist.edu.cn)

Received: 31 October 2023 – Discussion started: 20 November 2023

Revised: 7 January 2024 – Accepted: 12 January 2024 – Published: 21 February 2024

**Abstract.** The formation of secondary sulfate in the atmosphere remains controversial, and it is an urgent need to seek a new method to quantify different sulfate formation pathways. Thus, SO<sub>2</sub> and PM<sub>2.5</sub> samples were collected from 4 to 22 December 2019 in the Nanjing region. Sulfur and oxygen isotopic compositions were synchronously measured to study the contribution of SO<sub>2</sub> homogeneous and heterogeneous oxidation to sulfate. Meanwhile, the correlation of δ<sup>18</sup>O values between H<sub>2</sub>O and sulfate from SO<sub>2</sub> oxidation by H<sub>2</sub>O<sub>2</sub> and Fe<sup>3+</sup> / O<sub>2</sub> was simulatively investigated in the laboratory. Based on isotope mass equilibrium equations, the ratios of different SO<sub>2</sub> oxidation pathways were quantified. The results showed that secondary sulfate constituted higher than 80 % of total sulfate in PM<sub>2.5</sub> during the sampling period. Laboratory simulation experiments indicated that the δ<sup>18</sup>O value of sulfate was linearly dependent on the δ<sup>18</sup>O value of water, and the slopes of linear curves for SO<sub>2</sub> oxidation by H<sub>2</sub>O<sub>2</sub> and Fe<sup>3+</sup> / O<sub>2</sub> were 0.43 and 0.65, respectively. The secondary sulfate in PM<sub>2.5</sub> was mainly ascribed to SO<sub>2</sub> homogeneous oxidation by OH radicals and heterogeneous oxidation by H<sub>2</sub>O<sub>2</sub> and Fe<sup>3+</sup> / O<sub>2</sub>. SO<sub>2</sub> heterogeneous oxidation was generally dominant during sulfate formation, and SO<sub>2</sub> oxidation by H<sub>2</sub>O<sub>2</sub> predominated in SO<sub>2</sub> heterogeneous oxidation reactions, with an average ratio around 54.6 %. This study provided an insight into precisely evaluating sulfate formation by combining stable sulfur and oxygen isotopes.

## 1 Introduction

Sulfate is one of the prevalent components of PM<sub>2.5</sub> (Brügge-mann et al., 2021; Huang et al., 2014; Yang et al., 2023). Sulfate makes up approximately 25 % of PM<sub>2.5</sub> mass in Shanghai, 23 % in Guangzhou, and 10 %–33 % in Beijing (Xue et al., 2016). The rapid sulfate formation is a crucial factor determining the explosive growth of fine particles and the frequent occurrence of severe haze events in China (Lin et al., 2022; Y. Y. Liu et al., 2020; Meng et al., 2023; Wang et al., 2021; Zhang et al., 2018). Sulfate plays an important role in

the chemical and physical processes in the troposphere and lower stratosphere, and it significantly affects global climate change by scattering solar radiation and acting as cloud condensation nuclei (Gao et al., 2022; Ramanathan et al., 2001). Meanwhile, sulfate exerts a significant influence on air quality and public health (Abbatt et al., 2006).

In the past decades, numerous attempts have been made to evaluate SO<sub>2</sub> oxidation pathways that are involved in homogeneous and heterogeneous reactions. Traditionally, sulfate formation mechanisms mainly include SO<sub>2</sub> homogeneous oxidation by OH radicals and heterogeneous oxidation by

H<sub>2</sub>O<sub>2</sub>, O<sub>3</sub>, and O<sub>2</sub> catalysed by transition metal ions (TMIs) in cloud/fog water droplets. The relative importance of different sulfate formation pathways is strongly dependent on oxidant concentrations, the occurrence of fog/cloud events, and the pH of the aqueous phase (Kuang et al., 2022; Oh et al., 2023). Generally, SO<sub>2</sub> homogeneous oxidation by OH radicals and heterogeneous oxidation by H<sub>2</sub>O<sub>2</sub> are considered the most important pathways for sulfate production on the global scale (Seinfeld and Pandis, 1998). The photochemical reactivity during the winter in Beijing has been found to be relatively high, which favours the formation of reactive species such as OH radicals and H<sub>2</sub>O<sub>2</sub>, thereby facilitating SO<sub>2</sub> oxidation (Zhang et al., 2020). Xue et al. (2014) suggested that SO<sub>2</sub> oxidation by O<sub>3</sub> and H<sub>2</sub>O<sub>2</sub> in the aqueous phase contributed to the majority of total sulfate production. T. Liu et al. (2020) proposed that S(IV) oxidation by H<sub>2</sub>O<sub>2</sub> in aerosol water could be an important pathway that considers the ionic strength effect. He et al. (2018) found that the contribution of SO<sub>2</sub> oxidation by H<sub>2</sub>O<sub>2</sub> could reach 88 % during the haze period in Beijing. Ye et al. (2018) observed that the SO<sub>2</sub> oxidation rate by H<sub>2</sub>O<sub>2</sub> was 2–5 times faster than the summed rate of the other three oxidation pathways. As a result, the actual contribution of SO<sub>2</sub> oxidation by H<sub>2</sub>O<sub>2</sub> during the winter might be underestimated in the previous studies.

In addition, the presence of NO<sub>2</sub> is obviously favourable for SO<sub>2</sub> oxidation under the conditions of high relative humidity (RH) and NH<sub>3</sub>. NH<sub>3</sub> can promote the hydrolysis of NO<sub>2</sub> dimers to HONO and result in more sulfate formation on the particle surface in humid conditions (He et al., 2021). However, this conclusion was doubted by Liu et al. (2017), who believed that the reaction on actual fine particles with the pH at 4.2 was too slow to account for sulfate formation. Li et al. (2020) deemed that SO<sub>2</sub> oxidation by NO<sub>2</sub> might not be a major oxidation pathway in China. Furthermore, a GEOS-Chem modelling study suggested that NO<sub>2</sub> oxidation contributed less than 2 % of total sulfate production. It is found that the TMI pathway was very important in highly polluted regions, and the contribution of metal-catalysed SO<sub>2</sub> oxidation to sulfate was as high as 49 ± 10 % in haze. Wang et al. (2021) also argued that SO<sub>2</sub> oxidation via TMIs on the aerosol surface could be the dominant sulfate formation pathway. They found that manganese-catalysed oxidation of SO<sub>2</sub> contributed 69.2 ± 5.0 % of sulfate production. Overall, the mechanisms for sulfate rapid growth remain unclear and controversial. Therefore, sulfate formation pathways need to be further explored, and it is urgent that a new method to quantify different sulfate formation processes is developed.

Generally, sulfur isotopes allow for investigating SO<sub>2</sub> oxidation processes in the atmosphere because of distinctive isotope fractionation associated with different oxidation reactions (Harris et al., 2013). Harris et al. (2012) presented the respective sulfur isotope fractionation factors of SO<sub>2</sub> oxidation by OH radicals, O<sub>3</sub> / H<sub>2</sub>O<sub>2</sub>, and iron catalysis. In addition, the observed sulfur isotope fractionation of SO<sub>2</sub> oxidation by H<sub>2</sub>O<sub>2</sub> and O<sub>3</sub> appeared to have no significant dif-

ference. Therefore, the results were particularly useful to determine the importance of transition metal-catalysed oxidation pathway compared to other oxidation pathways. However, other main SO<sub>2</sub> oxidation pathways could not be distinguished only based on stable sulfur isotope determination.

The oxygen isotope ratio ( $\delta^{18}\text{O}$ ) can be used to deduce sulfate formation processes due to those SO<sub>2</sub> oxidation pathways affecting oxygen isotopes of the sulfate product differently. In particular, mass-independent fractionation signals of oxygen isotopes (nonzero  $\Delta^{17}\text{O}$ , where  $\Delta^{17}\text{O} = \delta^{18}\text{O} - 0.52 \times \delta^{17}\text{O}$ ) in sulfate are usually adopted to investigate the contribution of different SO<sub>2</sub> oxidation pathways. This method can identify the contribution of SO<sub>2</sub>+O<sub>3</sub> pathway when a high  $\Delta^{17}\text{O}$  value (> 3 ‰) is measured in sulfate. However, there is obvious uncertainty when interpreting the sulfate with a low  $\Delta^{17}\text{O}$  value (< 1 ‰). Unfortunately, most sulfate samples in the atmosphere present  $\Delta^{17}\text{O} < 1 \text{‰}$ , suggesting a limited contribution of the SO<sub>2</sub>+O<sub>3</sub> pathway during sulfate formation. It is noteworthy that the contribution of SO<sub>2</sub>+H<sub>2</sub>O<sub>2</sub> and TMI pathway is unclear if solely using  $\Delta^{17}\text{O}$  (Li et al., 2020). Holt and Kumar (1984) found that the use of oxygen isotopes was a valuable and complementary method to determine probable mechanisms of SO<sub>2</sub> oxidation to sulfate in the atmosphere. This provides us an insight into precisely evaluating sulfate formation pathways by combining oxygen and sulfur isotopes.

In this contribution, PM<sub>2.5</sub> and SO<sub>2</sub> were sampled from 4 to 22 December 2019 in Nanjing. Sulfur and oxygen isotopic compositions were measured to study the contribution of SO<sub>2</sub> homogeneous and heterogeneous oxidation during sulfate formation. In addition, the linear relationships of  $\delta^{18}\text{O}$  values between H<sub>2</sub>O and sulfate from SO<sub>2</sub> oxidation by H<sub>2</sub>O<sub>2</sub> and Fe<sup>3+</sup> / O<sub>2</sub> were synchronously investigated in the laboratory. Based on sulfur and oxygen isotope mass equilibrium equations, the ratios of different SO<sub>2</sub> oxidation pathways during the sampling period were calculated. The study aims to seek a novel method to quantify different SO<sub>2</sub> oxidation processes with sulfur and oxygen isotopes.

## 2 Materials and methods

### 2.1 Sampling location

PM<sub>2.5</sub> and SO<sub>2</sub> in the atmosphere were sampled from 4 to 22 December 2019 in Nanjing, China. The sampling site was located on the roof of the library of Nanjing University of Information Science and Technology (NUIST; 32.1° N, 118.5° E), which is depicted in Fig. 1. The sampling location is on the side of Ningliu Road and close to Nanjing chemical industry park. There are some large-scale chemical enterprises present such as Nanjing steel plant, Nanjing thermal power plants, and Nanjing petrochemical company, which inevitably release lots of SO<sub>2</sub> and iron metal into the atmosphere.

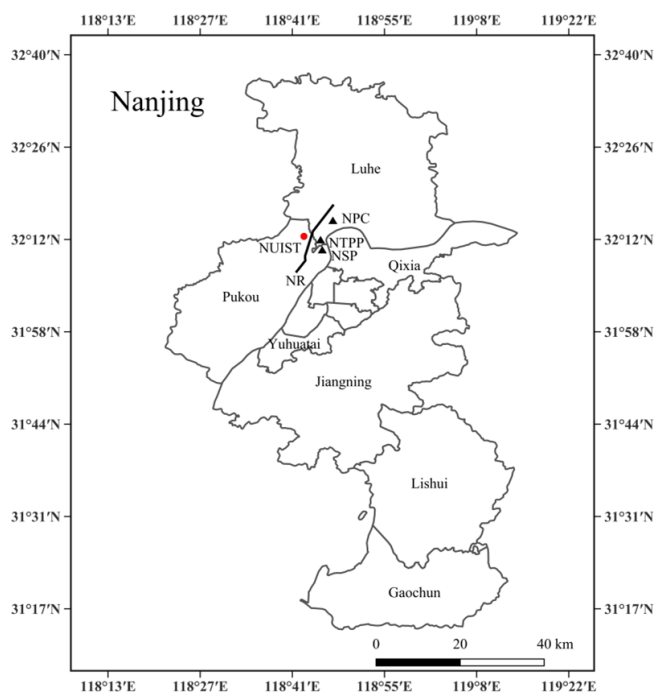


**Figure 1.** Sampling site of NUIST in Nanjing, China. NSP: Nanjing steel plant. NTTP: Nanjing thermal power plants. NPC: Nanjing petrochemical company. NR: Ningliu Road.

## 2.2 PM<sub>2.5</sub> and SO<sub>2</sub> samples collection

PM<sub>2.5</sub> and SO<sub>2</sub> were sampled using a modified JCH-1000 sampler (Juchuang Co., Qingdao) with a flow rate of 1.05 m<sup>3</sup> min<sup>-1</sup> from 08:00 to 20:00 from 4 to 22 December 2019. PM<sub>2.5</sub> and SO<sub>2</sub> were collected with a quartz filter (203 × 254 mm, Munktell, Sweden) and a glass fibre filter (203 × 254 mm, Tisch Environment INC, USA), respectively. The filters were incinerated in a muffle furnace at 450 °C for 2 h and then preserved in the desiccators at room temperature. The glass fibre filters were firstly soaked in 2 % K<sub>2</sub>CO<sub>3</sub> and 2 % glycerol solution for 2 h and dried in a DGG-9070A electric oven. SO<sub>2</sub> can be changed into sulfite immediately during the sampling.

## 2.3 Extractions of water-soluble sulfate

PM<sub>2.5</sub> sample filters were shredded and soaked in 400 mL of Milli-Q (18 MΩ) water for extractions of water-soluble sulfate. Filters were then isolated from solutions by centrifugation, and sulfate was precipitated as BaSO<sub>4</sub> by adding 1 mol L<sup>-1</sup> BaCl<sub>2</sub>. After the filtration with 0.22 μm acetate membrane, BaSO<sub>4</sub> precipitate was rinsed with Milli-Q water to remove Cl<sup>-</sup>. Finally, BaSO<sub>4</sub> powders were calcined at 800 °C for 2 h to obtain high-purity BaSO<sub>4</sub>. In addition, a small amount of H<sub>2</sub>O<sub>2</sub> solution was added to oxidize sulfite to sulfate.

## 2.4 Laboratory simulation of SO<sub>2</sub> oxidation by H<sub>2</sub>O<sub>2</sub> and Fe<sup>3+</sup> / O<sub>2</sub>

For SO<sub>2</sub> oxidation by H<sub>2</sub>O<sub>2</sub>, 30 mL min<sup>-1</sup> Ar was firstly introduced into three kinds of different water for about 30 min to drive out air. Sulfate was produced by adding 10 mL H<sub>2</sub>O<sub>2</sub> dilute solution (0.1 mL 30 % H<sub>2</sub>O<sub>2</sub> in 50 mL water) to SO<sub>2</sub> in the reaction chamber at 10 °C. H<sub>2</sub>O<sub>2</sub> solution was agitated vigorously for 1 min before admission of air. For SO<sub>2</sub> oxidation by Fe<sup>3+</sup> / O<sub>2</sub>, 2 mL min<sup>-1</sup> SO<sub>2</sub> and 2 mL min<sup>-1</sup> O<sub>2</sub> were simultaneously put into the Fe<sup>3+</sup> dilute solution at 10 °C. Then, 10 mL 1 mL min<sup>-1</sup> BaCl<sub>2</sub> was added to prepare BaSO<sub>4</sub>. Oxygen isotopic compositions of product sulfate and three kinds of water were measured to study their linear relationships.

## 2.5 Sulfur and oxygen isotope determination

Sulfur isotopic compositions in sulfate were analysed using an elemental analyser (EA; Flash 2000, Thermo) and isotope mass spectrometer (IRMS; Delta V Plus, Finnigan). High-purity BaSO<sub>4</sub> was converted into SO<sub>2</sub> in EA in the presence of Cu<sub>2</sub>O. SO<sub>2</sub> from EA was ionized, and the δ<sup>34</sup>S value was measured using the IRMS. For the determination of δ<sup>18</sup>O, BaSO<sub>4</sub> pyrolysis was conducted in a graphite furnace at 1450 °C, and the δ<sup>18</sup>O value was obtained in CO produced from the pyrolysis at continuous-flow mode. The results of δ<sup>34</sup>S and δ<sup>18</sup>O were with respect to the international standards V-CDT and V-SMOW, and the accuracy was better than ± 0.2 ‰ and ± 0.3 ‰, respectively.

## 3 Results and discussion

### 3.1 Concentrations of PM<sub>2.5</sub>, sulfate and SO<sub>2</sub>

As described in Fig. 2, the mass concentrations of PM<sub>2.5</sub>, SO<sub>4</sub><sup>2-</sup>, and SO<sub>2</sub> during the period from 4 to 22 December 2019 in NUIST changed from 28.1 to 67.0 μg m<sup>-3</sup>, 8.3 to 17.8 μg m<sup>-3</sup>, and 6.2 to 20.9 μg m<sup>-3</sup>, with an average and standard deviation at 45.7 ± 12.1, 12.7 ± 3.3 and 10.2 ± 4.4 μg m<sup>-3</sup>, respectively. It can be observed that PM<sub>2.5</sub> average concentration was about 1.3 times the First Grade National Ambient Air Quality Standard (35 μg m<sup>-3</sup>) and beyond the safety standard of the World Health Organization (10 μg m<sup>-3</sup>). The photochemical reactivity during the winter in Beijing has been found to be relatively high (Zhang et al., 2020), which facilitates the formation of some photooxidants. The relatively clean days during the sampling period indicate the importance of photoinduced oxidation of SO<sub>2</sub>.

Meanwhile, the change trends of PM<sub>2.5</sub>, SO<sub>4</sub><sup>2-</sup>, and SO<sub>2</sub> concentrations were found to be basically the same during the sampling period, indicating that sulfate was mainly from SO<sub>2</sub> oxidation. In particular, PM<sub>2.5</sub>, SO<sub>4</sub><sup>2-</sup>, and SO<sub>2</sub> concentrations increased to the maximum values on 10 December. It is noted that NO<sub>2</sub> and CO concentrations were 85 and

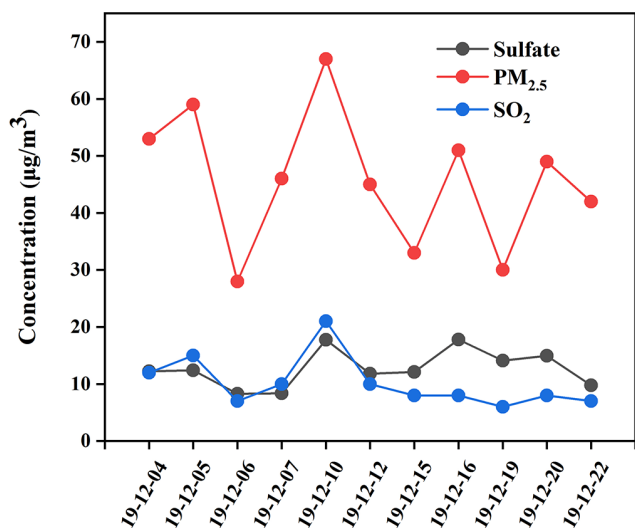


**Figure 2.** Variations in concentrations of PM<sub>2.5</sub>, SO<sub>4</sub><sup>2-</sup>, and SO<sub>2</sub>.

1.60 µg m<sup>-3</sup> on 10 December, which were also the maximum values during the sampling period. Based on the wind speed being lower than 3 m s<sup>-1</sup> and there being static weather during the sampling period, we believe that high CO concentration was mainly from local emissions. However, O<sub>3</sub> concentration on 10 December had a minimum value at 24 µg m<sup>-3</sup>, which preliminarily indicated that SO<sub>2</sub> oxidation by NO<sub>2</sub> might be a major pathway in sulfate formation. Previous studies showed that SO<sub>2</sub> oxidation by NO<sub>2</sub> in aerosol water dominated heterogeneous sulfate formation during wintertime at neutral aerosol pH (Wang et al., 2016; Cheng et al., 2016). However, subsequent studies showed that the calculated aerosol pH was in the range of 4.2–4.7, and the reactions between SO<sub>2</sub> and NO<sub>2</sub> during this pH range were too slow to produce sulfate. Considering low aerosol pH in the Nanjing region, we suggested that SO<sub>2</sub> oxidation by NO<sub>2</sub> was not a dominant pathway for sulfate formation during the sampling period.

In contrast, PM<sub>2.5</sub>, SO<sub>4</sub><sup>2-</sup>, and SO<sub>2</sub> concentrations were observed to be at minimum values on 6 December. Similarly, NO<sub>2</sub> and CO concentrations were also at minimum values of 36 and 0.6 mg m<sup>-3</sup>, respectively. However, O<sub>3</sub> concentration on 6 December had a maximum value at 50 µg m<sup>-3</sup>. In addition, the rate of SO<sub>2</sub> oxidation with O<sub>3</sub> becomes fast only when pH > 5, and the reaction rate of SO<sub>2</sub> with O<sub>3</sub> is one-hundredth of that with H<sub>2</sub>O<sub>2</sub> or TMIs when pH < 5. Therefore, pH values of actual fine particles at 4–5 in the Nanjing region could markedly restrain SO<sub>2</sub> oxidation by O<sub>3</sub>. The lowest SO<sub>4</sub><sup>2-</sup> concentration on 6 December further demonstrated that SO<sub>2</sub> oxidation by O<sub>3</sub> played an insignificant role in sulfate formation.

Generally, aqueous-phase oxidation is deemed to be a main process of sulfate formation in atmospheric environment. Shao et al. (2018) believed that heterogeneous sulfate

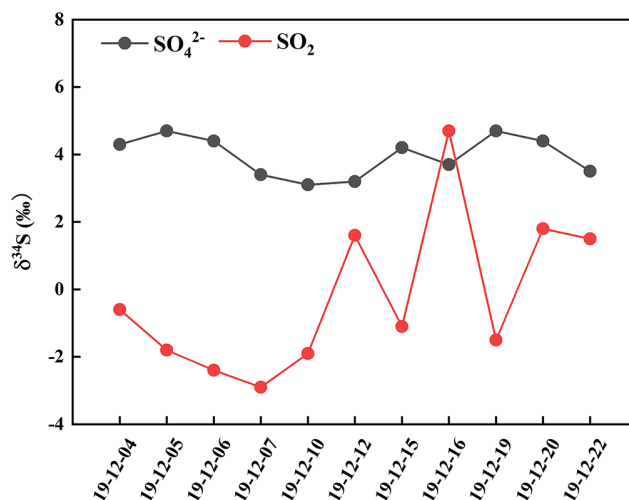


**Figure 3.** Variations in sulfur isotopic compositions in sulfate and SO<sub>2</sub>.

production on aerosols occurred when RH was higher than 50%. The RH values of the atmosphere ranging from 50.7% to 88.9% during the sampling period indicated that sulfate formation was closely related to SO<sub>2</sub> heterogeneous oxidation.

### 3.2 Sulfur isotopic compositions in sulfate and SO<sub>2</sub>

It can be observed from Fig. 3 that the values of δ<sup>34</sup>S-SO<sub>4</sub><sup>2-</sup> were generally higher compared to those of δ<sup>34</sup>S-SO<sub>2</sub> during the sampling period except on 16 December. The δ<sup>34</sup>S-SO<sub>4</sub><sup>2-</sup> values ranged from 3.1‰ to 4.7‰, with an average and standard deviation at 4.0 ± 0.6‰, while δ<sup>34</sup>S-SO<sub>2</sub> values changed from -2.9‰ to 4.7‰, with an average and standard deviation at -0.2 ± 2.3‰. The discrepancy between the values of δ<sup>34</sup>S-SO<sub>4</sub><sup>2-</sup> and δ<sup>34</sup>S-SO<sub>2</sub> was mainly related to the sulfur isotope fractionation effect during SO<sub>2</sub> oxidation to secondary sulfate.

It is noteworthy that δ<sup>34</sup>S-SO<sub>4</sub><sup>2-</sup> values were similar to those in PM<sub>2.5</sub>, with an average at 4.2‰ during the Youth Olympic Games in August 2014 in Nanjing (Guo et al., 2016). However, the average value of δ<sup>34</sup>S-SO<sub>4</sub><sup>2-</sup> during the sampling period was lower than 5.6‰ in Nanjing during a typical haze event from 21 December 2015 to 1 January 2016 (Guo et al., 2019). The higher δ<sup>34</sup>S values of sulfate in haze were possibly ascribed to SO<sub>2</sub> heterogeneous oxidation, which typically enriched heavy sulfur isotope in sulfate. In this study, the average concentrations of PM<sub>2.5</sub> were 45.7 µg m<sup>-3</sup>, indicating a time interval that is not heavily polluted. In addition, the relatively high temperature during the sampling period was favourable for photochemical reactions and OH radicals' formation. As a result, the contribution of SO<sub>2</sub> homogenous oxidation increased during sulfate formation, which enriched light sulfur isotope compared to that in haze. Han et al. (2017) determined δ<sup>34</sup>S values in Beijing

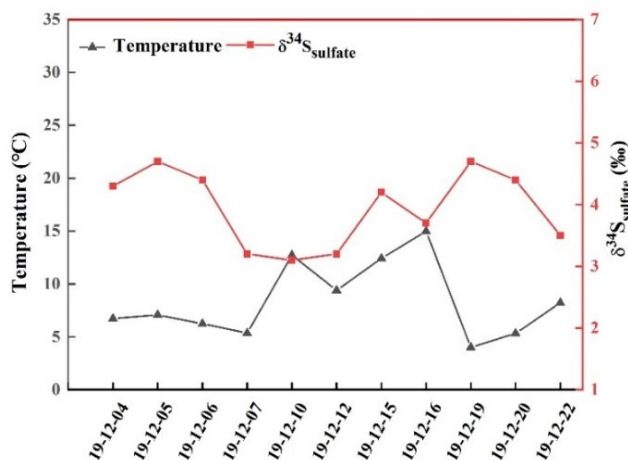


**Figure 4.** The correlation between  $\delta^{34}\text{S-SO}_4^{2-}$  values and atmospheric temperature.

PM<sub>2.5</sub>, with an average at 6.0‰. It is observed that there was a regional difference in  $\delta^{34}\text{S-SO}_4^{2-}$  values. The  $\delta^{34}\text{S-SO}_4^{2-}$  value in Nanjing was generally lower than that in Beijing. The discrepancy of  $\delta^{34}\text{S-SO}_4^{2-}$  value illustrated different sulfur sources and SO<sub>2</sub> oxidation pathways in these regions. In addition,  $\delta^{34}\text{S-SO}_4^{2-}$  values presented a seasonal change.  $\delta^{34}\text{S}$  values in Beijing aerosol sulfate varied from 3.4‰ to 7.0‰, with an average of 5.0‰ in summer, and from 7.1‰ to 11.3‰, with an average of 8.6‰ in winter. Generally, SO<sub>2</sub> homogeneous oxidation dominated in summer compared to that in winter due to strong solar irradiation (Han et al., 2016). SO<sub>2</sub> oxidation might lead to sulfur isotope fractionation, which was mainly attributed to equilibrium or kinetic discrimination between SO<sub>2</sub> and sulfate. The influence of different oxidants on sulfur isotope fractionation needed to be further investigated.

Figure 4 presents the relationship between the  $\delta^{34}\text{S-SO}_4^{2-}$  value and atmospheric temperature during the sampling period. It can be observed that there was an obviously negative correlation. The higher temperature generally corresponded to the lower  $\delta^{34}\text{S-SO}_4^{2-}$  value. This is mainly ascribed to the kinetic effect of sulfur isotope fractionation during SO<sub>2</sub> oxidation. At high temperature, more OH radicals were produced, and the contribution of SO<sub>2</sub> homogeneous oxidation increased. It is reported that sulfur isotope fractionation about SO<sub>2</sub> was −9‰ for homogeneous oxidation process (Tanaka et al., 1994). Therefore, a low  $\delta^{34}\text{S}$  value in sulfate at high temperature was chiefly due to the elevated SO<sub>2</sub> homogeneous oxidation.

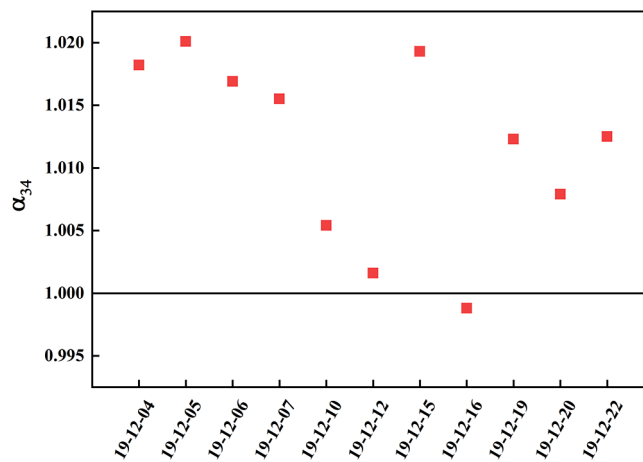


**Figure 5.** Sulfur isotope fractionation coefficients during SO<sub>2</sub> oxidation.

### 3.3 Sulfur isotope fractionation during SO<sub>2</sub> oxidation

The secondary sulfate was generally from SO<sub>2</sub> homogeneous and heterogeneous oxidation (Seinfeld and Pandis, 1998). The homogeneous and heterogeneous oxidation of SO<sub>2</sub> might lead to sulfur isotope fractionation, which is described using the fractionation coefficient: ( $\alpha$ )

$$\alpha = \frac{\frac{\delta^{34}\text{S}_{\text{SO}_4^{2-}}}{10^3} + 1}{\frac{\delta^{34}\text{S}_{\text{SO}_2}}{10^3} + 1} \quad (1)$$

Sulfate enriched heavy sulfur isotope ( $\alpha > 1$ ) during SO<sub>2</sub> heterogeneous oxidation for the presence of isotope equilibrium fractionation and kinetic fractionation. However, the light sulfur isotope enriched by sulfate ( $\alpha < 1$ ) during SO<sub>2</sub> homogeneous oxidation due to this process was only related to kinetic fractionation. As described in Fig. 5,  $\alpha$  values ranged from 0.9988 to 1.0201, indicating there was SO<sub>2</sub> homogeneous and heterogeneous oxidation during the sampling period. The  $\alpha$  value was at a minimum of 0.9988 on 16 December, which showed SO<sub>2</sub> homogeneous oxidation played a crucial role.

It is reported that the sulfur isotope fractionation during SO<sub>2</sub> heterogeneous and homogeneous oxidation to sulfate was 16.5‰ and −9‰, respectively (Tanaka et al., 1994). Consequently, the contribution of SO<sub>2</sub> heterogeneous and homogeneous oxidation to sulfate could be calculated by sulfur isotope mass equilibrium in Eqs. (2) and (3).

$$\delta^{34}\text{S}_{\text{SO}_2} + 16.5x - 9y = \delta^{34}\text{S}_{\text{SO}_4^{2-}} \quad (2)$$

$$x + y = 1, \quad (3)$$

where  $x$  and  $y$  represent the contribution of SO<sub>2</sub> heterogeneous and homogeneous oxidation, respectively.

It is observed from Fig. 6 that most of the days (7 out of 11) had more than 50% contributions from SO<sub>2</sub> heterogeneous oxidation, which indicated that SO<sub>2</sub> heterogeneous

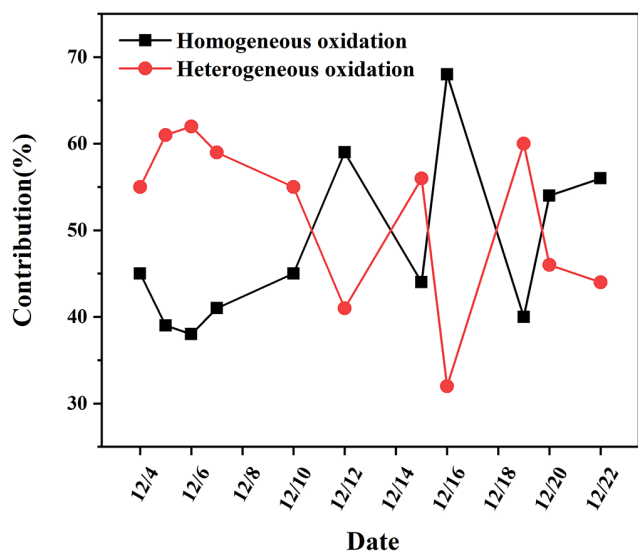


**Figure 6.** The contributions of SO<sub>2</sub> heterogeneous and homogeneous oxidation to sulfate.

oxidation was generally dominant during sulfate formation. He et al. (2018) presented the observations of oxygen-17 excess of PM<sub>2.5</sub> sulfate collected in Beijing haze from October 2014 to January 2015 and found the contribution of heterogeneous sulfate production was about 41%–54% with a mean of  $48 \pm 5\%$ . The contribution of SO<sub>2</sub> heterogeneous oxidation reached a high level during 5–7 December and on 19 December, which was closely related to the temperature of the atmosphere. The low temperature of about 5 °C during these days was favourable for SO<sub>2</sub> dissolution in water and further oxidized to sulfate. On 16 December, the contribution of SO<sub>2</sub> heterogeneous oxidation was at a minimum of 31.4%. The highest temperature of 15 °C on 16 December restrained SO<sub>2</sub> solubility in the aqueous solution and facilitated production of lots of gaseous oxidants such as OH radicals to promote SO<sub>2</sub> homogeneous oxidation.

Overall, the temperature was an important factor in controlling SO<sub>2</sub> oxidation pathways. High temperature facilitated kinetic fractionation of sulfur isotope during SO<sub>2</sub> oxidation to sulfate, thereby decreasing the  $\delta^{34}\text{S}$  value in sulfate. In addition, there was a lack of positive correlation between the contribution of SO<sub>2</sub> heterogeneous oxidation and O<sub>3</sub> or NO<sub>2</sub> concentration. This further demonstrated that SO<sub>2</sub> oxidation by O<sub>3</sub> and NO<sub>2</sub> was not an important pathway during the sampling period. Consequently, we mainly focused on SO<sub>2</sub> heterogeneous oxidation by H<sub>2</sub>O<sub>2</sub> and Fe<sup>3+</sup>/O<sub>2</sub> in the following study.

### 3.4 The correlation of $\delta^{18}\text{O}$ values between H<sub>2</sub>O and SO<sub>4</sub><sup>2-</sup> from SO<sub>2</sub> oxidation by H<sub>2</sub>O<sub>2</sub> and Fe<sup>3+</sup>/O<sub>2</sub>

It is known that SO<sub>2</sub> rapidly equilibrates with ambient water for very high molar ratios of H<sub>2</sub>O to SO<sub>2</sub> in the atmo-

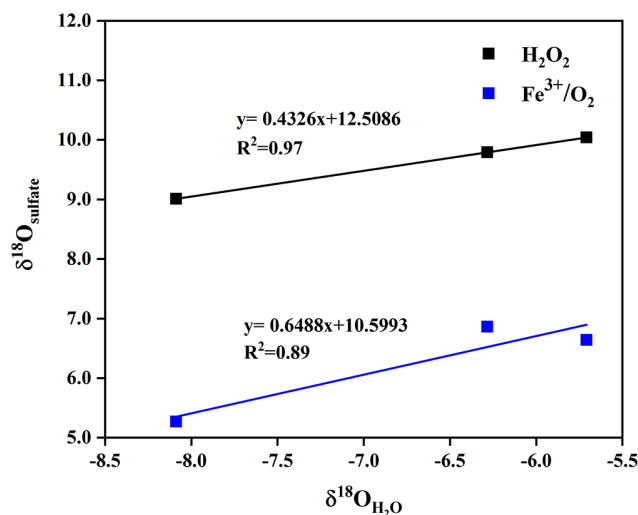


**Figure 7.** The correlation of  $\delta^{18}\text{O}$  values between H<sub>2</sub>O and sulfate from SO<sub>2</sub> oxidation by H<sub>2</sub>O<sub>2</sub> and Fe<sup>3+</sup>/O<sub>2</sub>, respectively.

sphere. As a result, the  $\delta^{18}\text{O}$  value of SO<sub>2</sub> is dynamically controlled by the  $\delta^{18}\text{O}$  value of water, and the  $\delta^{18}\text{O}$  value of SO<sub>2</sub> has no obvious effect on the  $\delta^{18}\text{O}$  value of sulfate produced from different oxidation pathways. Meanwhile, sulfate is very stable with respect to O atom exchange with ambient water. Consequently,  $\delta^{18}\text{O}$  can be adopted to distinguish SO<sub>2</sub> oxidation processes due to the  $\delta^{18}\text{O}$  value of product sulfate reflecting the distinctive signals of different oxidants.

We simulatively studied SO<sub>2</sub> heterogeneous oxidation by H<sub>2</sub>O<sub>2</sub> and Fe<sup>3+</sup>/O<sub>2</sub> in the laboratory, which aims to clarify the relationship of  $\delta^{18}\text{O}$  values between product sulfate and three kinds of water at 10 °C. It can be observed from Fig. 7 that the  $\delta^{18}\text{O}$  value of sulfate was linearly dependent on the  $\delta^{18}\text{O}$  value of water, and the slope of linear curve for H<sub>2</sub>O<sub>2</sub> oxidation approximates a ratio of 0.43, indicating that the isotopy of about two of four oxygen atoms in sulfate was controlled by the  $\delta^{18}\text{O}$  value of water. The other two oxygen atoms were from H<sub>2</sub>O<sub>2</sub> molecules, whose O–O bond remained intact during SO<sub>2</sub> oxidation. In addition, we noted from Fig. 7 that the slope of the linear curve for Fe<sup>3+</sup>/O<sub>2</sub> oxidation was about 0.65, which represented that the isotopy of about three of four oxygen atoms in sulfate was related to the  $\delta^{18}\text{O}$  value of water. A 3/4 control of sulfate oxygens by water is also characteristic of heterogeneous oxidation mechanisms in which HSO<sub>3</sub><sup>-</sup> isotopically equilibrated with water prior to significant oxidation to SO<sub>4</sub><sup>2-</sup>. The other one oxygen atom in sulfate was from O<sub>2</sub>. The higher slope suggested a higher dependence of the  $\delta^{18}\text{O}$  value of sulfate on the  $\delta^{18}\text{O}$  value of water during SO<sub>2</sub> heterogeneous oxidation by Fe<sup>3+</sup>/O<sub>2</sub>. The discrepancy of the slopes for different SO<sub>2</sub> heterogeneous oxidation processes provides us with a potential method to distinguish SO<sub>2</sub> oxidation pathways.

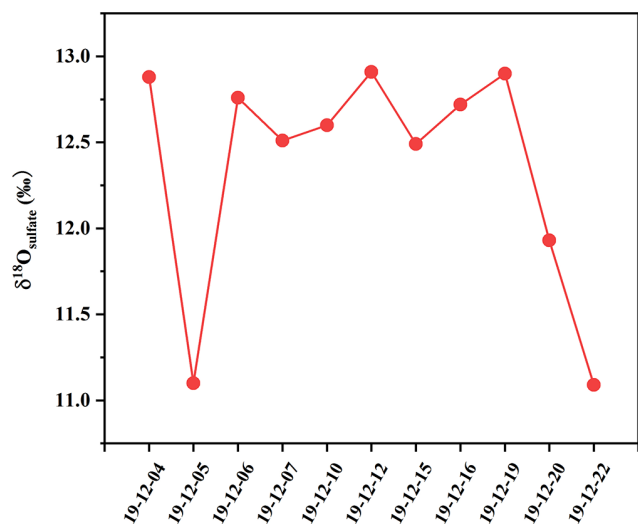


**Figure 8.**  $\delta^{18}\text{O}$  values of sulfate in  $\text{PM}_{2.5}$  during the sampling period.

### 3.5 $\delta^{18}\text{O}\text{-SO}_4^{2-}$ values in $\text{PM}_{2.5}$ and $\text{SO}_2$ main oxidation pathways

As depicted in Fig. 8,  $\delta^{18}\text{O}$  values of sulfate in  $\text{PM}_{2.5}$  ranged from 11.09‰ to 12.93‰, with an average and standard deviation of  $12.35 \pm 0.68$ ‰.  $\delta^{18}\text{O}$  values of sulfate focused on a narrow scope, except those on 5 and 22 December. It should be pointed out that the  $\delta^{18}\text{O}$  value of secondary sulfate was a comprehensive result from different  $\text{SO}_2$  oxidation processes. Sulfate in  $\text{PM}_{2.5}$  usually consisted of primary sulfate and secondary sulfate. The  $\delta^{18}\text{O}$  value of primary sulfate is about 38‰ (Holt and Kumar, 1984), which is significantly higher than the values of secondary sulfate. The contribution of primary and secondary sulfate in the atmosphere can be calculated by the oxygen isotope mass equilibrium in Eq. (4) (Ben et al., 1982):

$$\delta^{18}\text{O}_{\text{PM}_{2.5}} = \delta^{18}\text{O}_{\text{PS}} \times (1 - f_{\text{SS}}) + \delta^{18}\text{O}_{\text{SS}} \times f_{\text{SS}}, \quad (4)$$

where  $\delta^{18}\text{O}_{\text{PM}_{2.5}}$ ,  $\delta^{18}\text{O}_{\text{PS}}$ , and  $\delta^{18}\text{O}_{\text{SS}}$  mean  $\delta^{18}\text{O}$  values of  $\text{PM}_{2.5}$ , primary sulfate, and secondary sulfate, respectively, and  $f_{\text{SS}}$  is the contribution of secondary sulfate in  $\text{PM}_{2.5}$ .

It is noteworthy from Fig. 9 that there is a linear relationship between  $\delta^{18}\text{O}$  values in water and secondary sulfate from different  $\text{SO}_2$  oxidation pathways, and this can be described by Eqs. (5)–(7), where the value of  $\delta^{18}\text{O}_{\text{water}}$  is about  $-6.2$ ‰ in the Nanjing region. As discussed above, secondary sulfate was mainly ascribed to  $\text{SO}_2$  homogeneous oxidation by OH radicals and heterogeneous oxidation by  $\text{H}_2\text{O}_2$  and  $\text{Fe}^{3+}/\text{O}_2$ . Therefore, the  $\delta^{18}\text{O}_{\text{SS}}$  value in Eq. (4) can be obtained based on Eqs. (5)–(7), respectively. As a result, the average contribution of primary and secondary sulfate in  $\text{PM}_{2.5}$  is presented in Table 1. It can be observed that the majority of sulfate in  $\text{PM}_{2.5}$  was secondary sulfate, which appears to constitute from 79.9% to 86.2% of total sulfate

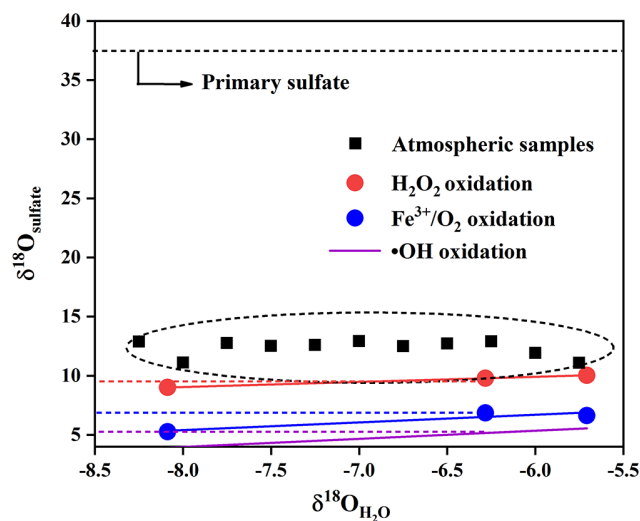


**Figure 9.** The correlation between  $\delta^{18}\text{O}$  values in water and sulfate in  $\text{PM}_{2.5}$ .

**Table 1.** The average contribution of primary sulfate and secondary sulfate in  $\text{PM}_{2.5}$ .

Sampling time	Primary sulfate (%)	Secondary sulfate (%)
4 December	19.7	80.3
5 December	13.9	86.1
6 December	19.3	80.7
7 December	18.4	81.6
10 December	18.7	81.3
12 December	20.0	80.0
15 December	18.4	81.6
16 December	20.1	79.9
19 December	19.7	80.3
20 December	16.7	83.3
22 December	13.8	86.2

during the sampling period. It is admirable to quantitatively describe these formation pathways of secondary sulfate in  $\text{PM}_{2.5}$ .

$$\delta^{18}\text{O}_{\text{SS}} = 0.69 \times \delta^{18}\text{O}_{\text{water}} + 9.5\text{‰ (OH)} \quad (\text{Holt and Kumar, 1984}) \quad (5)$$

$$\delta^{18}\text{O}_{\text{SS}} = 0.65 \times \delta^{18}\text{O}_{\text{water}} + 10.6\text{‰ (Fe}^{3+}/\text{O}_2) \quad (\text{this study}) \quad (6)$$

$$\delta^{18}\text{O}_{\text{SS}} = 0.43 \times \delta^{18}\text{O}_{\text{water}} + 12.5\text{‰ (H}_2\text{O}_2) \quad (\text{this study}) \quad (7)$$

According to the percentages of  $\text{SO}_2$  heterogeneous and homogeneous oxidation to sulfate in Fig. 6 and the average contributions of primary sulfate and secondary sulfate in

**Table 2.** The ratios of SO<sub>2</sub> different oxidation pathways to sulfate.

Time	$f_{SS-OH}$	$f_{SS-H_2O_2}$	$f_{SS-Fe_3+/O_2}$	$f_{SS-H_2O_2}/$ ( $f_{SS-H_2O_2} +$ $f_{SS-Fe_3+/O_2}$ ) (%)
4 December	0.45	0.27	0.28	49.1
5 December	0.39	0.24	0.37	39.3
6 December	0.38	0.24	0.38	38.7
7 December	0.41	0.25	0.34	42.3
10 December	0.45	0.27	0.28	49.1
12 December	0.59	0.30	0.11	73.2
15 December	0.44	0.26	0.30	46.5
16 December	0.68	0.26	0.06	81.2
19 December	0.40	0.25	0.35	41.6
20 December	0.54	0.31	0.15	67.4
22 December	0.56	0.32	0.12	72.7

PM<sub>2.5</sub> in Table 1, we can further calculate the ratios of different SO<sub>2</sub> oxidation pathways at 10 °C via the oxygen isotope mass equilibrium in Eqs. (8)–(10), and the corresponding results are depicted in Table 2.

$$\delta^{18}O_{PM_{2.5}} = \delta^{18}O_{PS} \times f_{PS} + \left( \delta^{18}O_{SS-OH} \times f_{SS-OH} + \delta^{18}O_{SS-Fe_3+/O_2} \times f_{SS-Fe_3+/O_2} + \delta^{18}O_{SS-H_2O_2} \times f_{SS-H_2O_2} \right) \times f_{SS} \quad (8)$$

$$f_{PS} + f_{SS} = 1 \quad (9)$$

$$f_{SS-OH} + f_{SS-Fe_3+/O_2} + f_{SS-H_2O_2} = 1, \quad (10)$$

where  $\delta^{18}O_{PM_{2.5}}$  and  $\delta^{18}O_{PS}$  are  $\delta^{18}O$  values of total sulfate and primary sulfate in PM<sub>2.5</sub>;  $\delta^{18}O_{SS-OH}$ ,  $\delta^{18}O_{SS-Fe_3+/O_2}$  and  $\delta^{18}O_{SS-H_2O_2}$  are  $\delta^{18}O$  values of secondary sulfate from SO<sub>2</sub> oxidation by OH radicals, Fe<sup>3+</sup>/O<sub>2</sub>, and H<sub>2</sub>O<sub>2</sub>, respectively;  $f_{PS}$  and  $f_{SS}$  are the contribution of primary and secondary sulfate; and  $f_{SS-OH}$ ,  $f_{SS-Fe_3+/O_2}$ , and  $f_{SS-H_2O_2}$  are the ratios of secondary sulfate from SO<sub>2</sub> oxidation by OH radicals, Fe<sup>3+</sup>/O<sub>2</sub>, and H<sub>2</sub>O<sub>2</sub>, respectively.

Unlike heavily polluted days with reduced solar irradiation, the photochemical reactivity can remain high in clean days during the observation period because of relatively intense solar irradiation. As a result, some photochemical reactive species such as OH radicals and H<sub>2</sub>O<sub>2</sub> are deemed to be the major oxidants for sulfate formation. Generally, H<sub>2</sub>O<sub>2</sub> production in the relatively clean atmosphere is ascribed to self-reaction of HO<sub>2</sub> radicals that mainly comes from the reactions of OH radicals with CO and volatile organic compounds. It is observed from Table 2 that the ratios of SO<sub>2</sub> oxidation by OH radicals ranged from 38 % to 68 %, with an average and standard deviation at 48 ± 9.7 %. The ratio reached the maximum of 68 % on 16 December, which is mainly ascribed to the highest temperature of 15 °C during the sam-

pling period. The photochemical reactions are favourable for producing more OH radicals. In contrast, the ratio of SO<sub>2</sub> oxidation by OH radicals decreased to the minimum of 38 % on 6 December due to the low temperature.

It is known that SO<sub>2</sub> oxidation by H<sub>2</sub>O<sub>2</sub> and Fe<sup>3+</sup>/O<sub>2</sub> is the most important pathway during SO<sub>2</sub> heterogeneous oxidation. It can be observed from Table 2 that the percentage of sulfate from SO<sub>2</sub> oxidation by H<sub>2</sub>O<sub>2</sub> in secondary sulfate from SO<sub>2</sub> heterogeneous oxidation changed from 38.7 % to 81.2 %, with an average and standard deviation at 54.6 ± 15.7 %, indicating that SO<sub>2</sub> oxidation by H<sub>2</sub>O<sub>2</sub> predominated during SO<sub>2</sub> heterogeneous oxidation. In addition, there was an obviously positive correlation between the ratios of SO<sub>2</sub> oxidation by H<sub>2</sub>O<sub>2</sub> and OH radicals, which was chiefly attributed to the photochemical reactions. The relatively strong solar irradiation on 16 December resulted in the maximum ratio of 81.2 % for H<sub>2</sub>O<sub>2</sub> oxidation in SO<sub>2</sub> heterogeneous reactions. The sampling site is close to Nanjing steel plant. As companion emitters, Fe<sup>3+</sup> is present in much higher concentrations than that in other areas. It is believed that SO<sub>2</sub> oxidation by O<sub>2</sub> in the presence of Fe<sup>3+</sup> was not negligent in the areas where the concentrations of SO<sub>2</sub> and Fe<sup>3+</sup> were high. This inevitably resulted in the high SO<sub>2</sub> oxidation ratio by Fe<sup>3+</sup>/O<sub>2</sub> in SO<sub>2</sub> heterogeneous oxidation processes.

## 4 Conclusions

There was no serious PM<sub>2.5</sub> pollution during the sampling period. The secondary sulfate constitutes from 79.9 % to 86.2 % of total sulfate in PM<sub>2.5</sub>. SO<sub>2</sub> oxidation by O<sub>3</sub> and NO<sub>2</sub> played an insignificant role in sulfate formation. The secondary sulfate was mainly ascribed to SO<sub>2</sub> homogeneous oxidation by OH radicals and heterogeneous oxidation by H<sub>2</sub>O<sub>2</sub> and Fe<sup>3+</sup>/O<sub>2</sub>. Compared to homogeneous oxidation, SO<sub>2</sub> heterogeneous oxidation was generally dominant, with an average contribution of 51.6 %. SO<sub>2</sub> oxidation by H<sub>2</sub>O<sub>2</sub>



predominated in SO<sub>2</sub> heterogeneous oxidation reactions, the average ratio of which reached 54.6%. Consequently, sulfur and oxygen isotopes can be used to gain an insight into sulfate formation. The determination of sulfur isotopic compositions in SO<sub>2</sub> and sulfate is advantageous in quantifying the contribution of SO<sub>2</sub> homogeneous and heterogeneous oxidation. Combining field observations of oxygen isotope in the atmosphere with the linear relationships of  $\delta^{18}\text{O}$  values between H<sub>2</sub>O and sulfate from different SO<sub>2</sub> oxidation processes can obtain an increased understanding of specific sulfate formation pathways. This study is favourable for deeply investigating the sulfur cycle in the atmosphere.

**Data availability.** Data supporting this paper are available upon request from the corresponding author (guocumt@nuist.edu.cn).

**Author contributions.** ZiG carried out the experiment and wrote the original draft. KL designed the methodology and administrated the project. PQ and MX performed the data collection. ZhG instructed the experiment and revised the paper.

**Competing interests.** The contact author has declared that none of the authors has any competing interests.

**Disclaimer.** Publisher's note: Copernicus Publications remains neutral with regard to jurisdictional claims made in the text, published maps, institutional affiliations, or any other geographical representation in this paper. While Copernicus Publications makes every effort to include appropriate place names, the final responsibility lies with the authors.

**Acknowledgements.** We gratefully acknowledge the financial support from the National Natural Science Foundation of China (nos. 41873016, 51908294, and 21976006) and the National Science Fund for Distinguished Young Scholars (no. 22325601).

**Financial support.** This research has been supported by the National Natural Science Foundation of China (grant nos. 41873016, 51908294, and 21976006) and the National Science Fund for Distinguished Young Scholars (grant no. 22325601).

**Review statement.** This paper was edited by Zhibin Wang and reviewed by two anonymous referees.

## References

Abbatt, J. P. D., Benz, S., Cziczo, D. J., Kanji, Z., Lohmann, U., and Mohler, O.: Solid ammonium sulfate aerosols as ice nuclei:

- a pathway for cirrus cloud formation, *Science*, 313, 1770–1773, <https://doi.org/10.1126/science.1129726>, 2006.
- Ben, D. H., Romesh, K., and Paul, T. C.: Primary Sulfates in Atmospheric Sulfates: Estimation by Oxygen Isotope Ratio Measurements, *Science*, 217, 51–53, <https://doi.org/10.1126/science.217.4554.51>, 1982.
- Brüggemann, M., Riva, M., Perrier, S., Poulain, L., George, C., and Herrmann, H.: Overestimation of Monoterpene Organosulfate Abundance in Aerosol Particles by Sampling in the Presence of SO<sub>2</sub>, *Environ. Sci. Technol. Lett.*, 8, 206–211, <https://doi.org/10.1021/acs.estlett.0c00814>, 2021.
- Cheng, Y. F., Zheng, G. J., Wei, C., Mu, Q., Zheng, B., Wang, Z. B., Gao, M., Zhang, Q., He, K. B., Carmichael, G., Pöschl, U., and Su, H.: Reactive Nitrogen Chemistry in Aerosol Water as a Source of Sulfate during Haze Events in China, *Sci. Adv.*, 2, e1601530, <https://doi.org/10.1126/sciadv.1601530>, 2016.
- Gao, J., Wei, Y., Zhao, H., Liang, D., Feng, Y., and Shi, G.: The role of source emissions in sulfate formation pathways based on chemical thermodynamics and kinetics model, *Sci. Total. Environ.*, 851, 158104, <https://doi.org/10.1016/j.scitotenv.2022.158104>, 2022.
- Guo, Z. B., Shi, L., Chen, S. L., Jiang, W. J., Wei, Y., Rui, M. L., and Zeng, G.: Sulfur isotopic fractionation and source apportionment of PM<sub>2.5</sub> in Nanjing region around the second session of the Youth Olympic Games, *Atmos. Res.*, 174/175, 9–17, <https://doi.org/10.1016/j.atmosres.2016.01.011>, 2016.
- Guo, Z. Y., Guo, Q. J., Chen, S. L., Zhu, B., Zhang, Y., Yu, J., and Guo, Z. B.: Study on pollution behavior and sulfate formation during the typical haze event in Nanjing with water soluble inorganic ions and sulfur isotopes, *Atmos. Res.*, 217, 198–207, <https://doi.org/10.1016/j.atmosres.2018.11.009>, 2019.
- Han, X. K., Guo, Q. J., Liu, C. Q., Fu, P. Q., Strauss, H., Yang, J., Jian, H., Wei, L., Hong, R., Peters, M., Wei, R. F., and Tian, L.: Using stable isotopes to trace sources and formation processes of sulfate aerosols from Beijing, China, *Sci. Rep.*, 6, 29958, <https://doi.org/10.1038/srep29958>, 2016.
- Han, X. K., Guo, Q. J., Strauss, H., Liu, C. Q., Hu, J., Guo, Z. B., Wei, R. F., Peters, M., Tian, L., and Kong, J.: Multiple Sulfur Isotope Constraints on Sources and Formation Processes of Sulfate in Beijing PM<sub>2.5</sub> Aerosol, *Environ. Sci. Technol.*, 51, 7794–7803, <https://doi.org/10.1021/acs.est.7b00280>, 2017.
- Harris, E., Sinha, B., Hoppe, P., and Ono, S.: High-precision measurements of <sup>33</sup>S and <sup>34</sup>S fractionation during SO<sub>2</sub> oxidation reveal causes of seasonality in SO<sub>2</sub> and sulfate isotopic composition, *Environ. Sci. Technol.*, 47, 12174–12183, <https://doi.org/10.1021/es402824c>, 2013.
- Harris, E., Sinha, B., Hoppe, P., Crowley, J. N., Ono, S., and Foley, S.: Sulfur isotope fractionation during oxidation of sulfur dioxide: gas-phase oxidation by OH radicals and aqueous oxidation by H<sub>2</sub>O<sub>2</sub>, O<sub>3</sub> and iron catalysis, *Atmos. Chem. Phys.*, 12, 407–424, <https://doi.org/10.5194/acp-12-407-2012>, 2012.
- He, P. Z., Alexander, B., Geng, L., Chi, X. Y., Fan, S. D., Zhan, H. C., Kang, H., Zheng, G. J., Cheng, Y. F., Su, H., Liu, C., and Xie, Z. Q.: Isotopic constraints on heterogeneous sulfate production in Beijing haze, *Atmos. Chem. Phys.*, 18, 5515–5528, <https://doi.org/10.5194/acp-18-5515-2018>, 2018.
- He, X., Wu, J. J., Ma, Z. C., Xi, X., and Zhang, Y. H.: NH<sub>3</sub>-promoted heterogeneous reaction of SO<sub>2</sub> to sulfate on  $\alpha$ -Fe<sub>2</sub>O<sub>3</sub> particles with coexistence of NO<sub>2</sub> under dif-

- ferent relative humidities, *Atmos. Environ.*, 262, 118622, <https://doi.org/10.1016/j.atmosenv.2021.118622>, 2021.
- Holt, B. D. and Kumar, R.: Oxygen-18 study of high-temperature air oxidation of SO<sub>2</sub>, *Atmos. Environ.*, 18, 2089–2094, [https://doi.org/10.1016/0004-6981\(84\)90194-X](https://doi.org/10.1016/0004-6981(84)90194-X), 1984.
- Huang, R. J., Zhang, Y., Bozzetti, C., Ho, K. F., Cao, J. J., Han, Y., Daellenbach, K. R., Slowik, J. G., Platt, S. M., Canonaco, F., Zotter, P., Wolf, R., Pieber, S. M., Bruns, E. A., Crippa, M., Ciarelli, G., Piazzalunga, A., Schwikowski, M., Abbaszade, G., Schnelle-Kreis, J., Zimmermann, R., An, Z., Szidat, S., Baltensperger, U., El Haddad, I., and Prevot, A. S.: High secondary aerosol contribution to particulate pollution during haze events in China, *Nature*, 514, 218–222, <https://doi.org/10.1038/nature13774>, 2014.
- Kuang, B., Zhang, F., Shen, J., Shen, Y., Qu, F., Jin, L., Tang, Q., Tian, X., and Wang, Z.: Chemical characterization, formation mechanisms and source apportionment of PM<sub>2.5</sub> in north Zhejiang Province: The importance of secondary formation and vehicle emission, *Sci. Total. Environ.*, 851, 158206, <https://doi.org/10.1016/j.scitotenv.2022.158206>, 2022.
- Li, J. H. Y., Zhang, Y. L., Cao, F., Zhang, W., and Michalski, G.: Stable Sulfur Isotopes Revealed a Major Role of Transition-Metal Ion-Catalyzed SO<sub>2</sub> Oxidation in Haze Episodes, *Environ. Sci. Technol.*, 54, 2626–2634, <https://doi.org/10.1021/acs.est.9b07150>, 2020.
- Lin, Y. C., Yu, M., Xie, F., and Zhang, Y.: Anthropogenic Emission Sources of Sulfate Aerosols in Hangzhou, East China: Insights from Isotope Techniques with Consideration of Fractionation Effects between Gas-to-Particle Transformations, *Environ. Sci. Technol.*, 56, 3905–3914, <https://doi.org/10.1021/acs.est.1c05823>, 2022.
- Liu, M. X., Song, Y., Zhou, T., Xu, Z. Y., Yan, C. Q., Zheng, M., Wu, Z. J., Hu, M., Wu, Y. S., and Zhu, T.: Fine particle pH during severe haze episodes in northern China, *Geophys. Res. Lett.*, 44, 5213–5221, <https://doi.org/10.1002/2017GL073210>, 2017.
- Liu, T., Clegg, S. L., and Abbatt, J. P. D.: Fast oxidation of sulfur dioxide by hydrogen peroxide in deliquesced aerosol particles, *P. Natl Acad. Sci. USA*, 117, 1354–1359, <https://doi.org/10.1073/pnas.1916401117>, 2020.
- Liu, Y. Y., Wang, T., Fang, X. Z., Deng, Y., Cheng, H. Y., Nabi, I., and Zhang, L.: Brown carbon: An underlying driving force for rapid atmospheric sulfate formation and haze event, *Sci. Total. Environ.*, 734, 139415, <https://doi.org/10.1016/j.scitotenv.2020.139415>, 2020.
- Meng, X., Hang, Y., Lin, X., Li, T. T., Wang, T. J., Cao, J. J., Fu, Q. Y., Dey, S., Huang, K., Liang, F. C., Kan, H. D., Shi, X. M., and Liu, Y.: A satellite-driven model to estimate long-term particulate sulfate levels and attributable mortality burden in China, *Environ. Int.*, 171, 107740, <https://doi.org/10.1016/j.envint.2023.107740>, 2023.
- Oh, S. H., Park, K., Park, M., Song, M., Jang, K. S., Schauer, J. J., Bae, G. N., and Bae, M. S.: Comparison of the sources and oxidative potential of PM<sub>2.5</sub> during winter time in large cities in China and South Korea, *Sci. Total. Environ.*, 859, 160369, <https://doi.org/10.1016/j.scitotenv.2022.160369>, 2023.
- Ramanathan, V., Crutzen, P. J., Kiehl, J. T., and Rosenfeld, D.: Aerosols, climate, and the hydrological cycle, *Science*, 294, 2119–2124, <https://doi.org/10.1126/science.1064034>, 2001.
- Seinfeld, J. H. and Pandis, S. N.: *Atmospheric Chemistry and Physics: From Air Pollution to Climate Change*, *Phys. Today*, 51, 88–90, <https://doi.org/10.1063/1.882420>, 1998.
- Shao, J. Y., Chen, Q. J., Wang, Y. X., Lu, X., He, P. Z., Sun, Y. L., Shah, V., Martin, R. V., Philip, S., Song, S. J., Zhao, Y., Xie, Z. Q., Zhang, L., and Alexander, B.: Heterogeneous sulfate aerosol formation mechanisms during wintertime Chinese haze events: air quality model assessment using observations of sulfate oxygen isotopes in Beijing, *Atmos. Chem. Phys.*, 19, 6107–6123, <https://doi.org/10.5194/acp-19-6107-2019>, 2019.
- Tanaka, N., Rye, D. M., Xiao, Y., and Lassaga, A. C.: Use of stable sulfur isotope systematic for evaluating oxidation reaction pathways and in-cloud scavenging of sulfur dioxide in the atmosphere, *Geophys. Res. Lett.*, 21, 1519–1522, <https://doi.org/10.1029/94GL00893>, 1994.
- Wang, G. H., Zhang, R. Y., Gomez, M. E., Yang, L. X., Levy Zamora, M., Hu, M., Lin, Y., Peng, J. F., Guo, S., Meng, J. J., Li, J. J., Cheng, C. L., Hu, T. F., Ren, Y. Q., Wang, Y. S., Gao, J., Cao, J. J., An, Z. S., Zhou, W. J., Li, G. H., Wang, J. Y., Tian, P. F., Marrero-Ortiz, W., Secret, J., Du, Z. F., Zheng, J., Shang, D. J., Zeng, L. M., Shao, M., Wang, W. G., Huang, Y., Wang, Y., Zhu, Y. J., Li, Y. X., Hu, J. X., Pan, B., Cai, L., Cheng, Y. T., Ji, Y. M., Zhang, F., Rosenfeld, D., Liss, P. S., Duce, R. A., Kolb, C. E., and Molina, M. J.: Persistent sulfate formation from London Fog to Chinese haze, *P. Natl. Acad. Sci. USA*, 113, 13630–13635, <https://doi.org/10.1073/pnas.1616540113>, 2016.
- Wang, W. G., Liu, M. Y., Wang, T. T., Song, Y., Zhou, L., Cao, J. J., Zhu, T., Tian, H. Z., and Ge, M. F.: Sulfate formation is dominated by manganese-catalyzed oxidation of SO<sub>2</sub> on aerosol surfaces during haze events, *Nat. Commun.*, 12, 1993, <https://doi.org/10.1038/s41467-021-22091-6>, 2021.
- Xue, J., Yuan, Z., Yu, J. Z., and Lau, A. K. H.: An Observation-Based Model for Secondary Inorganic Aerosols, *Aerosol Air Qual. Res.*, 14, 862–878, <https://doi.org/10.4209/aaqr.2013.06.0188>, 2014.
- Xue, J., Yuan, Z., Griffith, S. M., Yu, X., Lau, A. K. H., and Yu, J. Z.: Sulfate Formation Enhanced by a Cocktail of High NO<sub>x</sub>, SO<sub>2</sub>, Particulate Matter, and Droplet pH during Haze-Fog Events in Megacities in China: An Observation-Based Modeling Investigation, *Environ. Sci. Technol.*, 50, 7325–7334, <https://doi.org/10.1021/acs.est.6b00768>, 2016.
- Yang, T., Xu, Y., Ye, Q., Ma, Y. J., Wang, Y. C., Yu, J. Z., Duan, Y. S., Li, C. X., Xiao, H. W., Li, Z. Y., Zhao, Y., and Xiao, H. Y.: Spatial and diurnal variations of aerosol organosulfates in summertime Shanghai, China: potential influence of photochemical processes and anthropogenic sulfate pollution, *Atmos. Chem. Phys.*, 23, 13433–13450, <https://doi.org/10.5194/acp-23-13433-2023>, 2023.
- Ye, C., Liu, P. F., Ma, Z. B., Xue, C. Y., Zhang, C. L., Zhang, Y. Y., Liu, J. F., Liu, C. T., Sun, X., and Mu, Y. J.: High H<sub>2</sub>O<sub>2</sub> Concentrations Observed during Haze Periods during the Winter in Beijing: Importance of H<sub>2</sub>O<sub>2</sub> Oxidation in Sulfate Formation, *Environ. Sci. Technol. Lett.*, 5, 757–763, <https://doi.org/10.1021/acs.estlett.8b00579>, 2018.
- Zhang, R., Sun, X. S., Shi, A. J., Huang, Y. H., Yan, J., Nie, T., Yan, X., and Li, X.: Secondary inorganic aerosols formation during haze episodes at an urban site in Beijing, China, *Atmos. Environ.*, 177, 275–282, <https://doi.org/10.1016/j.jes.2022.01.008>, 2018.

Zhang, Y., Bao, F. X., Li, M., Xia, H. L., Huang, D., Chen C. C., and Zhao, J. C.: Photoinduced Uptake and Oxidation of SO<sub>2</sub> on Beijing Urban PM<sub>2.5</sub>, *Environ. Sci. Technol.*, 54, 14868–14876, <https://doi.org/10.1021/acs.est.0c01532>, 2020.